

Inflammatory Cytokines and Hypoxia Contribute to ^{18}F -FDG Uptake by Cells Involved in Pannus Formation in Rheumatoid Arthritis

Tamiko Matsui¹, Norihito Nakata¹, Shigenori Nagai^{2,3}, Akira Nakatani¹, Miwako Takahashi⁴, Toshimitsu Momose⁴, Kuni Ohtomo⁴, and Shigeo Koyasu²

¹Research Center, Nihon Medi-physics Co., Ltd., Chiba, Japan; ²Department of Microbiology and Immunology, Keio University School of Medicine, Tokyo, Japan; ³Core Research for Evolutional Science and Technology, Japan Science and Technology Agency, Tokyo, Japan; and ⁴Department of Radiology, Graduate School of Medicine, The University of Tokyo, Tokyo, Japan

Assessment of the activity of rheumatoid arthritis (RA) is important for the prediction of future articular destruction. ^{18}F -FDG PET is known to represent the metabolic activity of inflammatory disease, which correlates with the pannus volume measured by MRI or ultrasonography. To evaluate the correlation between ^{18}F -FDG accumulation and RA pathology, we assessed ^{18}F -FDG accumulation in vivo using collagen-induced arthritis (CIA) animal models and ^3H -FDG uptake in vitro using various cells involved in arthritis. **Methods:** ^{18}F -FDG PET images of rats with CIA were acquired on days 10, 14, and 17 after arthritis induction. The specimens were subsequently subjected to macroautoradiography, and the ^{18}F -FDG accumulation was compared with the histologic findings. ^3H -FDG uptake in vitro in inflammatory cells (neutrophils, macrophages, T cells, and fibroblasts) was measured to evaluate the contributions of these cells to ^{18}F -FDG accumulation. In addition, the influence on ^3H -FDG uptake of inflammatory factors, such as cytokines (tumor necrosis factor α [TNF α], interleukin 1 [IL-1], and IL-6), and hypoxia was examined. **Results:** ^{18}F -FDG PET depicted swollen joints, and ^{18}F -FDG accumulation increased with the progression of arthritis. Histologically, a higher level of ^{18}F -FDG accumulation correlated with the pannus rather than the infiltration of inflammatory cells around the joints. In the in vitro ^3H -FDG uptake assay, fibroblasts showed the highest ^3H -FDG uptake, followed by neutrophils. Although only a small amount of ^3H -FDG was incorporated by resting macrophages, a dramatic increase in ^3H -FDG uptake in both fibroblasts and macrophages was observed when these cells were exposed to inflammatory cytokines, such as TNF α and IL-1, and hypoxia. Although neutrophils showed relatively high ^3H -FDG uptake without activation, no increase in ^3H -FDG uptake was observed in response to inflammatory cytokines. ^3H -FDG uptake by T cells was much lower than that by other cells. Thus, fibroblasts and activated macrophages contribute to a

high level of ^{18}F -FDG accumulation in the pannus, and hypoxia as well as cytokine stimulation significantly increases ^{18}F -FDG uptake by these cells. **Conclusion:** ^{18}F -FDG accumulation in RA reflects proliferating pannus and inflammatory activity enhanced by inflammatory cytokines and hypoxia. ^{18}F -FDG PET should be effective for quantifying the inflammatory activity of RA.

Key Words: ^{18}F -FDG; rheumatoid arthritis; fibroblast; cytokine; hypoxia

J Nucl Med 2009; 50:920–926

DOI: 10.2967/jnumed.108.060103

Rheumatoid arthritis (RA) is an autoimmune disorder of unknown etiology and is characterized by systematic, symmetric, and erosive synovitis (1). RA synovitis shows massive leukocyte infiltration, proliferative synovial membranes, and neovascularization, which give rise to a synovial hypertrophy called a pannus. Such pannus formation is directly responsible for cartilage and bone destruction (2,3).

It recently became clear that the erosive changes of bone appear very early in RA (4), that the treatment of RA should start as early as possible, and that RA must be controlled adequately to reduce the occurrence of irreversible joint damage (5). Therefore, the early identification of pathologic synovitis and the appropriate monitoring of RA disease activity are important for the control of RA. However, current assessments of RA activity are not sufficient for appropriate monitoring. The conventional estimation of clinical features, such as joint tenderness and swelling, are relatively subjective, and laboratory examinations, such as the erythrocyte sedimentation rate (ESR) and serum C-reactive protein level, show just the mean value of the systemic inflammatory state. Radiography is unable to directly evaluate synovial inflammation before bone destruction (6).

Received Nov. 27, 2008; revision accepted Feb. 11, 2009.

For correspondence or reprints contact either of the following:

Akira Nakatani, Research Center, Nihon Medi-physics Co., Ltd., Kitasode 3-1, Sodegaura, Chiba 299-0266, Japan.

E-mail: akira_nakatani@nmp.co.jp

Shigeo Koyasu, Department of Microbiology and Immunology, Keio University School of Medicine, 35 Shinanomachi, Shinjuku-ku, Tokyo 160-8585, Japan.

koyasu@sc.itc.keio.ac.jp

COPYRIGHT © 2009 by the Society of Nuclear Medicine, Inc.

For overcoming these problems, some imaging modalities are capable of quantifying the activity of synovitis in each joint; these include MRI, high-resolution ultrasonography (US), and PET (7–9). PET imaging with ^{18}F -FDG, which is a glucose analog that reflects glucose metabolism, has been widely used in clinical oncology (10). Lately, it has been shown that ^{18}F -FDG PET can be applied to the evaluation of inflammatory diseases. For RA, it has been reported that ^{18}F -FDG uptake represents the metabolic activity of synovitis (8). Furthermore, correlations among the ^{18}F -FDG accumulation in synovitis, the volume of the pannus evaluated by MRI or US, and the therapeutic response have been shown (7,9,11). In addition, an advantage of ^{18}F -FDG PET is that whole-body ^{18}F -FDG PET can evaluate the activity of synovitis in all joints in a single examination (12).

However, the mechanisms of how ^{18}F -FDG accumulates in the inflammatory region, what types of cells play a major role in incorporating ^{18}F -FDG, and how inflammatory reactions affect the accumulation of ^{18}F -FDG are largely unknown. In this study, we examined the mechanisms of ^{18}F -FDG accumulation by using a murine collagen-induced arthritis (CIA) model in vivo and ^3H -FDG uptake by various cell types in vitro. We also examined the effects of inflammatory cytokines and hypoxia, both of which are known to affect the characteristics of various cells in inflammation. Our results show that both macrophages and fibroblasts play a major role in the uptake of ^3H -FDG and that inflammatory cytokines and hypoxia greatly enhance ^3H -FDG uptake in vitro, which likely reflects ^{18}F -FDG uptake in vivo.

MATERIALS AND METHODS

Preparation of CIA Model

Six-week-old female Lewis rats were purchased from Japan SLC and housed under constant environmental conditions with 12-h light–dark cycles. Food and water were provided ad libitum. Arthritis was induced according to the protocol recommended by Chondrex Inc., the supplier of bovine type II collagen. In brief, collagen (2 mg/mL) was mixed with an equal volume of *N*-acetylmuramyl-L-alanyl-D-isoglutamine hydrate (MDP; 8 mg/mL; Sigma). The collagen–MDP solution was emulsified with an equal volume of incomplete Freund adjuvant (Sigma) by stirring with an electric homogenizer. Rats were injected intradermally in the base of the tail with 0.3 mL of the emulsion of collagen–MDP–incomplete Freund adjuvant. The severity of arthritis in each paw was evaluated according to the following scale: 0 = no swelling or redness (normal paw); 1 = swelling or redness in digits; 2 = focal swelling or redness in digits and paw; 3 = swelling in entire paw; and 4 = severe swelling in entire paw. Animals that did not receive collagen injections were used as controls.

^{18}F -FDG PET

All rats were fasted for 16–20 h before the experiments but had free access to water. After thiopental sodium anesthesia (40 mg/kg intraperitoneally), rats were injected in the tail vein with 37 MBq (1.0 mCi) of ^{18}F -FDG (Nihon Medi-physics). Forty minutes after ^{18}F -FDG injection, emission scans were performed for 10 min with a small-animal PET scanner (eXplore Vista DR; GE Health-

care). The PET images were reconstructed by use of a 2-dimensional ordered-subset expectation maximization algorithm with 32 subsets, 2 iterations, random and scatter corrections, and no attenuation correction.

Macroautoradiography and Histologic Analysis

Rats were sacrificed 1 h after the ^{18}F -FDG injection (i.e., 10 min after the PET scan). Frozen sections of joints were prepared by use of the film method developed by Kawamoto et al. (13). In brief, hind paws were frozen in liquid nitrogen and embedded in cryoembedding medium (Finetec). Adhesive film (Cryofilm; Finetec) was attached to the exposed surface of frozen samples, and 10- μm -thick sections were cut with a cryostat (CM3050S-10; Leica Instruments) and mounted on glass slides. For macroautoradiography, the slides were exposed to imaging plates (BAS-SR 2040; Fuji Film) overnight. The imaging plates were then scanned with an imaging analyzer (BAS-2500; Fuji Film). Sections were then stained with hematoxylin and eosin (HE) for histologic evaluation. Immunohistochemical staining was performed on sections of day 17 samples. Contiguous sections were incubated with an anti-rat CD68 antibody (BMA Biomedicals) and an anti-rat granulocyte antibody (BD Biosciences Pharmingen) overnight at 4°C. Bound antibodies were detected with an LSAB2 Streptavidin-HRP (Dako) and 3,3'-diaminobenzidine tetrahydrochloride.

Preparation of Cells

Six-week-old male C57BL/6 mice were purchased from Japan SLC. Bone marrow cells collected from femurs were suspended in serum-free RPMI 1640 medium, and red blood cells were removed by use of the Lymphosepar (Immuno-Biologic Laboratories) density gradient method according to the manufacturer's recommendations. Mononuclear cells were cultured with 10 nM mouse macrophage–colony-stimulating factor (M-CSF; R&D) in RPMI 1640 culture medium supplemented with 10% fetal calf serum, 55 μM 2-mercaptoethanol, penicillin at 100 U/mL, streptomycin at 100 $\mu\text{g}/\text{mL}$, nonessential amino acids (Invitrogen), 1 mM sodium pyruvate, and 10 mM *N*-2-hydroxyethylpiperazine-*N'*-(2-ethanesulfonic acid) (pH 7.4) at 37°C in a 5% CO_2 humidified incubator. After 24 h of cultivation, nonadherent cells were collected and cultured for an additional 7 d in culture medium containing 40 nM M-CSF. Adherent cells were collected as bone marrow–derived macrophages and used for experiments.

Neutrophils were obtained from bone marrow cells by Histopaque (Sigma) density gradient centrifugation. Histopaque 1.083 was added on top of Histopaque 1.119, and the cell suspension was placed on the upper layer and centrifuged at 700g for 30 min at room temperature. This method routinely yielded nonprimed and viable neutrophils with greater than 85% purity.

Fibroblasts were isolated from dermal tissues. The back skin of a C57BL/6 mouse was washed with 70% ethanol, and the epidermis and dermis were separated physically after digestion with 0.3% (w/v) trypsin for 60 min at 37°C. The dermal samples were cut into small (2- to 3-mm) square pieces, and a few skin pieces were incubated under glass cover slips in a 6-well plate with RPMI 1640 culture medium. When fibroblast outgrowth became confluent, the cover slips and skin pieces were removed, and fibroblasts were collected with 0.25% trypsin–ethylenediaminetetraacetic acid at room temperature.

T cells were purified from splenocytes with anti–mouse CD90-conjugated magnetic beads (Miltenyi Biotec) and Auto MACS

(Miltenyi Biotec) according to the manufacturer's instructions. T cells were activated with concanavalin A (Con A) at 4 $\mu\text{g}/\text{mL}$ and cultured for 7 d to prepare preactivated T cells in a resting state.

Measurement of ^3H -FDG Uptake

^3H -FDG uptake in vitro was examined with 3.7 kBq of 5,6- ^3H -FDG (American Radiolabeled Chemicals) in assay medium (serum- and glucose-free RPMI 1640 medium, pH 7.4) for 1 h at 37°C. The effects of inflammatory cytokines on ^3H -FDG uptake were evaluated with the following cytokines: tumor necrosis factor α (TNF α ; 100 ng/mL; R&D), interleukin 1 β (IL-1 β ; 1,000 U/mL; R&D), and IL-6 (100 ng/mL; PeproTech). We also used phorbol myristate acetate (PMA; 10 ng/mL; Sigma), a known activator of neutrophils. Macrophages (2×10^5 cells/300 $\mu\text{L}/2 \text{ cm}^2$) and fibroblasts (5×10^4 cells/300 $\mu\text{L}/2 \text{ cm}^2$) were incubated in culture medium with or without cytokines for 24 h, and then the culture media were replaced with 500 μL of assay medium. Neutrophils (5×10^5 cells/500 $\mu\text{L}/1.5\text{-mL}$ tube) were incubated in assay medium with or without stimulation.

After incubation with ^3H -FDG, uptake was terminated with 3 washes of cold phosphate-buffered saline. The cells were then solubilized with 0.9 mL of 1N NaOH and neutralized with 0.9 mL of 1N HCl. Radioactivity was determined by use of a liquid scintillation counter (Tri-CARB 3100; Perkin-Elmer). The uptake of ^3H -FDG was calculated from the ratio of ^3H -FDG associated with the cell pellet to the initial dose (percentage injected dose [%ID]) and was normalized to living cell numbers (%ID/ 10^5 cells).

For hypoxia treatment, the cells were cultured in a humidified multigas incubator (APM-30DR; Astec) with 1% O_2 (hypoxia) and 5% CO_2 at 37°C for 24 h. Assay medium was preequilibrated overnight before use. Cells cultured in normoxia (20.9% O_2) were used as controls.

Statistics

All values are expressed as the mean \pm SD of multiple independent experiments. The data were evaluated statistically with the Mann-Whitney U test. Differences were considered significant when the P value was less than 0.05.

RESULTS

^{18}F -FDG Accumulation in CIA Model In Vivo

To evaluate how ^{18}F -FDG PET depicts arthritis during the progress of the disease, PET and macroautoradiography

of rats with CIA were performed at various days after the induction of arthritis. Rats developed arthritis at about day 14 after collagen injection and developed severe swelling of the joints by day 17 (Supplemental Fig. 1) (supplemental materials are available online only at <http://jnm.snmjournals.org>). We examined ^{18}F -FDG uptake in the joints by ^{18}F -FDG PET, and representative images are shown in the top row of Figure 1. The PET image of rats with CIA on day 10 was indistinguishable from that of control rats and revealed no marked ^{18}F -FDG accumulation in their joints. On day 14, when the disease symptoms were readily recognized, the swollen joints were clearly visualized by PET. The accumulation of ^{18}F -FDG in the tarsal joints was further increased by day 17, the later stage of the disease. These results indicated that ^{18}F -FDG PET is able to depict inflamed joints and that ^{18}F -FDG accumulation increases with the progression of arthritis.

We performed macroautoradiography of the joints after obtaining PET images (Fig. 1, middle row). Specimens on day 14 showed the focal accumulation of ^{18}F -FDG around the joints, and those on day 17 showed a high level of accumulation of ^{18}F -FDG at the advanced arthritis region (Fig. 1, middle row). Histologic analyses (Fig. 1, bottom row) revealed no significant changes in the joints 10 d after collagen injection. Rats with CIA on day 14 showed synovial cell hyperplasia with edema and interstitial infiltration of inflammatory cells—mainly neutrophils and macrophages. On day 17, pannus consisting of mixed cellular patterns of macrophages and fibroblasts were observed, and bone destruction by mature osteoclasts was often observed (Fig. 1, bottom row). Similar results were obtained with the CIA mouse model (Supplemental Fig. 2).

^{18}F -FDG Accumulation in Regions of Pannus and Bone Destruction

When we compared the histologic findings with ^{18}F -FDG accumulation in detail, the areas with a high level of ^{18}F -FDG accumulation (Fig. 2A, arrow) corresponded to the regions of pannus and bone destruction (Fig. 2B). In contrast, the areas with a moderate level of ^{18}F -FDG accumulation (Fig. 2A, arrowhead) corresponded to synovial cell hyperplasia and edematous inflammation (Fig. 2E).

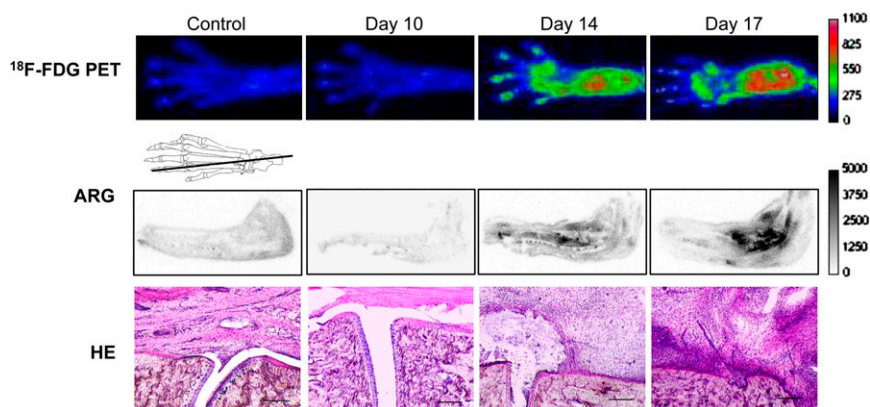


FIGURE 1. ^{18}F -FDG PET images of CIA animal model. PET images acquired 40 min after injection of 37 MBq of ^{18}F -FDG into rats with CIA (top row), macroautoradiograms (ARG) of sagittal sections (middle row), and HE staining of tarsometatarsal joints (bottom row) are shown. Images represent control rat and rats with CIA 10, 14, and 17 d after collagen injection. Bar = 200 μm .

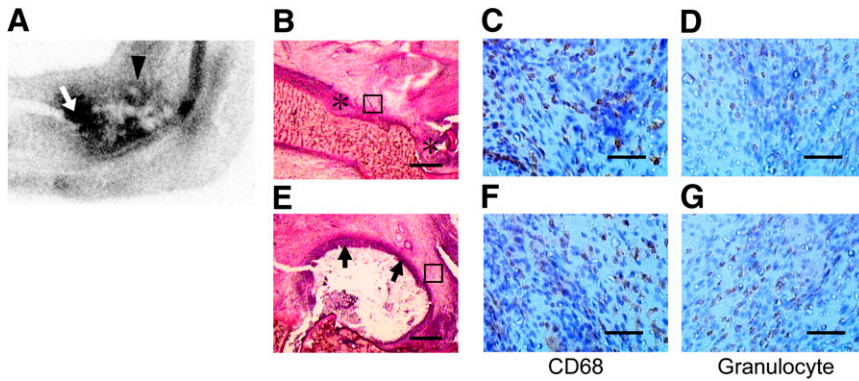


FIGURE 2. Immunohistochemical analyses of joints affected by CIA. (A) Macroautoradiogram of rat with CIA 17 d after collagen injection. (B and E) HE staining in region with high level of ^{18}F -FDG accumulation (B, arrow) and region with moderate level of ^{18}F -FDG accumulation (E, arrowhead in A). Asterisk in B shows bone destruction with pannus. Arrows in E show synovial cell hyperplasia. Bar = 500 μm . (C, D, F, and G) Representative immunohistochemical staining of serial sections for CD68 (C and F) and granulocytes (D and G). Data are from region with high level of ^{18}F -FDG

accumulation (C and D; enlarged view of square in B) and region with moderate level of ^{18}F -FDG accumulation (F and G; enlarged view of square in E). Bar = 50 μm .

These observations indicated that the distribution of ^{18}F -FDG corresponds to inflammatory regions, such as those with pannus formation and the infiltration of inflammatory cells. A high level of ^{18}F -FDG accumulation especially tends to correlate with severe pannus formation and considerable bone destruction.

Immunohistochemical staining was performed to examine the contributions of inflammatory cells to ^{18}F -FDG accumulation. Neutrophils and macrophages were readily observed to similar degrees in areas with both high and moderate levels of ^{18}F -FDG accumulation (Figs. 2C, 2D, 2F, and 2G), suggesting that the number of inflammatory cells may not be the major cause of localized ^{18}F -FDG accumulation in tissues with arthritis. It is possible that the difference in ^{18}F -FDG accumulation is attributable to the presence of fibroblasts as a constituent of the pannus. Alternatively, the increase in glucose metabolism observed with inflammatory cells may occur in a distinct microenvironment. For example, stimulation of arthritis with local

cytokines or hypoxia may cause a high level of accumulation of ^{18}F -FDG.

^3H -FDG Uptake by Various Cells In Vitro

To examine the factors affecting ^{18}F -FDG uptake by various cell types involved in the pathogenesis of RA (macrophages, neutrophils, fibroblasts, and T cells) in vivo, we performed a series of experiments with ^3H -FDG to evaluate the ability of various cells to incorporate ^{18}F -FDG and the effects of various inflammatory cytokines (TNF α , IL-1, and IL-6) in vitro. Preincubation of macrophages with TNF α resulted in a large increase in ^3H -FDG uptake (TNF α , 0.56 ± 0.25 %ID/ 10^5 cells; control, 0.11 ± 0.05 %ID/ 10^5 cells; $P < 0.05$), whereas IL-1 and IL-6 had little effect (Fig. 3A). For fibroblasts, stimulation by TNF α or IL-1 significantly increased ^3H -FDG uptake (TNF α , 2.21 ± 0.24 %ID/ 10^5 cells; IL-1, 1.71 ± 0.21 %ID/ 10^5 cells; control, 0.93 ± 0.16 %ID/ 10^5 cells; $P < 0.05$) (Fig. 3C). In contrast, the incubation of neutrophils (5×10^5

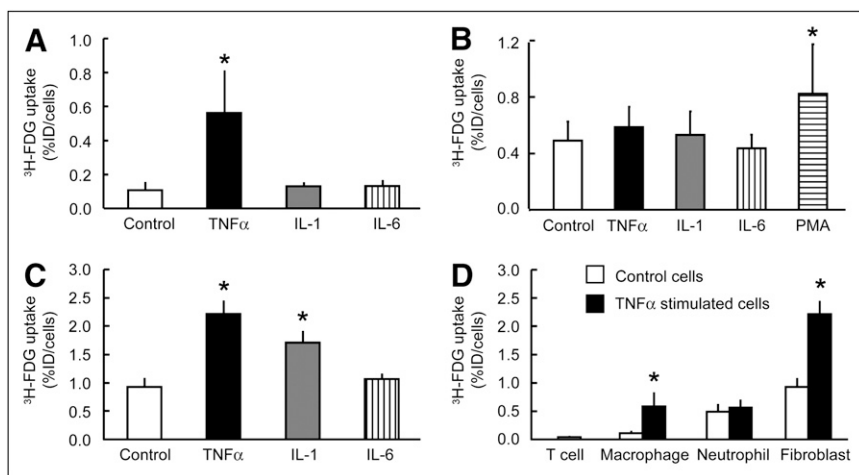


FIGURE 3. ^3H -FDG uptake in vitro and effects of inflammatory cytokines. (A–C) Effects of inflammatory cytokines on ^3H -FDG uptake in macrophages (A), neutrophils (B), and fibroblasts (C). Macrophages and fibroblasts were cultured with TNF α (100 ng/mL), IL-1 (1,000 U/mL), or IL-6 (100 ng/mL) for 24 h and then incubated with ^3H -FDG for 1 h. Neutrophils were incubated with ^3H -FDG for 1 h along with TNF α (100 ng/mL), IL-1 (1,000 U/mL), IL-6 (100 ng/mL), or PMA (10 ng/mL). ^3H -FDG uptake was normalized to numbers of living cells. Data represent mean \pm SD of percentage of uptake of initial dose per 10^5 cells in 3 separate experiments. (D) Comparison of ^3H -

FDG uptake in different types of cells. * $P < 0.05$ for comparison with control ($n = 3$ for each group), as determined by Mann-Whitney U test.

cells per tube) with TNF α , IL-1, or IL-6 for 1 h resulted in no significant increase in ^3H -FDG uptake, whereas a significant increase in ^3H -FDG uptake was observed when neutrophils were stimulated with the phorbol ester PMA (PMA, 0.82 ± 0.35 %ID/ 10^5 cells; control, 0.49 ± 0.14 %ID/ 10^5 cells; $P < 0.05$) (Fig. 3B). These results indicated that ^3H -FDG uptake by neutrophils is not significantly affected by these inflammatory cytokines. ^3H -FDG uptake by both naive T cells and T cells preactivated with Con A for 7 d was very low compared with that observed with other inflammatory cells (Fig. 3D and data not shown).

^3H -FDG uptake was highest for fibroblasts (0.93 ± 0.16 %ID/ 10^5 cells), followed by neutrophils (0.49 ± 0.14 %ID/ 10^5 cells), macrophages (0.11 ± 0.05 %ID/ 10^5 cells), and T cells (0.03 ± 0.0 %ID/ 10^5 cells) (Fig. 3D). These results indicated that fibroblasts significantly contribute to ^{18}F -FDG uptake and that inflammatory cytokines, such as TNF α , significantly enhance ^{18}F -FDG uptake by fibroblasts and macrophages.

Hypoxia Enhances ^3H -FDG Uptake

Because it is known that inflammatory areas, including those in RA, are hypoxic compared with noninflammatory areas (14–16), we examined the effect of hypoxia on ^3H -FDG uptake by various cells (Fig. 4). Under hypoxic conditions, ^3H -FDG uptake by macrophages (hypoxia, 1.2 ± 0.42 %ID/ 10^5 cells; normoxia, 0.29 ± 0.31 %ID/ 10^5 cells; $P < 0.05$) (Fig. 4A) and fibroblasts (hypoxia, 10.03 ± 2.27 %ID/ 10^5 cells; normoxia, 1.62 ± 0.38 %ID/ 10^5 cells; $P < 0.05$) (Fig. 4B) was significantly increased. ^3H -FDG uptake was further enhanced by TNF α stimulation under hypoxic conditions for macrophages (hypoxia, 3.53 ± 1.43 %ID/ 10^5 cells; normoxia, 1.20 ± 0.42 %ID/ 10^5 cells; $P < 0.05$) and fibroblasts (hypoxia, 16.65 ± 4.17 %ID/ 10^5 cells; normoxia, 10.03 ± 2.27 %ID/ 10^5 cells; $P < 0.05$) (Fig. 4). Interestingly, ^3H -FDG uptake by neutrophils was not enhanced under hypoxic conditions (data not shown). These results indicated that hypoxia as well as cytokine stimulation signif-

icantly increases ^3H -FDG uptake by macrophages and fibroblasts.

DISCUSSION

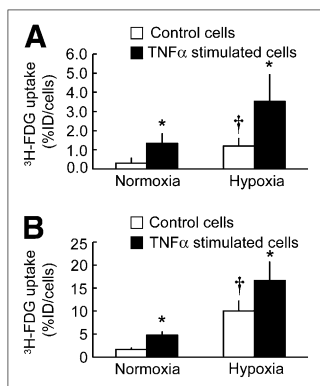
It was previously shown that ^{18}F -FDG can be used to assess the activity of rheumatoid synovitis and that the standardized uptake value is closely correlated with the volume of the enhancing pannus or the synovial thickness evaluated by MRI and US (7,9,11). However, it has not been clear what pathologic condition of RA ^{18}F -FDG reflects. In the present study, animal models of arthritis was used to show that ^{18}F -FDG accumulation in arthritis correlated with the active pannus. Fibroblasts showed the highest level of ^3H -FDG uptake among the various cell types forming the pannus. Our results also demonstrated that ^3H -FDG uptake was increased in the presence of proinflammatory cytokines. It has been shown that TNF α and IL-1 induce the cell cycle progression of fibroblasts (17,18). In fact, synovial fibroblasts in joints affected by RA showed increased proliferative activity and increased glycolysis compared with those in normal joints (19,20). Fibroblast proliferation may be one of the dominant causes of ^{18}F -FDG accumulation in vivo. Thus, it is suggested that fibroblasts play a key role in ^{18}F -FDG accumulation in arthritis.

Previous studies suggested that neutrophils and macrophages contribute to ^{18}F -FDG accumulation mainly in inflammatory diseases (17,21). Indeed, although only a small amount of ^3H -FDG was incorporated by resting macrophages, a dramatic increase in ^3H -FDG uptake was observed on stimulation with TNF α . Activated macrophages thus contribute to ^{18}F -FDG accumulation in RA. In contrast, neutrophils showed a relatively high level of ^3H -FDG uptake without activation, but inflammatory cytokines had little influence on the ^3H -FDG uptake. These results indicate that the contribution of neutrophils to ^{18}F -FDG accumulation depends simply on the amount of cell infiltration and does not reflect the activity of inflammatory cytokines.

On the basis of our results, it is likely that abundant cytokine production in RA is one of the characteristic conditions that affect ^{18}F -FDG uptake. TNF α , IL-1, and IL-6 are known to be the major cytokines involved in the process of RA. These cytokines are produced by synovio-cytes and mononuclear cells and activate inflammatory cells as well as fibroblasts (18,22). The energy to support the inflammatory activities enhanced by these cytokines is supplied primarily by glucose metabolism, as the depletion of glucose from the medium easily gives rise to a severe depression of IL-1 production from stimulated macrophages (23).

In addition to the production of inflammatory cytokines, another characteristic of RA is hypoxia. The dysfunction of the neovascular network in RA fails to maintain tissue oxygen homeostasis, and intense inflammation induces

FIGURE 4. Effects of hypoxia on ^3H -FDG uptake in macrophages (A) and fibroblasts (B). Macrophages and fibroblasts were incubated in absence (open bars) or presence (filled bars) of TNF α (100 ng/mL) in normoxia (20.9% O $_2$) or hypoxia (1% O $_2$) for 24 h. Cells were then incubated with ^3H -FDG for 1 h. Data represent mean \pm SD of 3 separate experiments. * $P < 0.05$ in comparison with nonstimulated control ($n = 3$); † $P < 0.05$ in comparison with nonstimulated sample in normoxia ($n = 3$). P values were determined by Mann-Whitney U test.



marked hypoxia in joints affected by RA (14–16). We showed here that hypoxia is another condition that enhances the uptake of ^{18}F -FDG by both macrophages and fibroblasts. Hypoxia changes the energy supply of cells into anaerobic glycolysis. According to studies of glucose use by macrophages, differences in O_2 tension lead to alterations in the rate of oxidative phosphorylation and glycolysis, and hypoxia upregulates glucose uptake and lactate production (24,25). Furthermore, it is known that macrophages regulate many factors associated not only with survival, such as the glucose transporter and vascular endothelial growth factor, but also inflammation, such as $\text{TNF}\alpha$ and IL-1, under hypoxic conditions (26). Cellular activation induced by hypoxia is a critical factor that complicates synovitis and increases ^{18}F -FDG accumulation in RA. In contrast, because neutrophils are thought to provide glycolytic substrates from intracellular glycogen in the presence of low glucose levels, it is possible that ^3H -FDG uptake in neutrophils is not affected by activation under experimental conditions (27,28).

For human RA, fewer neutrophils but large numbers of T cells and B cells infiltrate the pannus; this pattern is different from the observations in the CIA animal model. The CIA animal model shows a pathologically acute inflammatory condition associated with marked neutrophil invasion; this pattern is rare in human RA. Because of the involvement of fewer neutrophils in human RA, it is believed that ^{18}F -FDG PET can depict the proliferating pannus more specifically. In contrast, to fibroblasts the level of ^3H -FDG uptake by T cells preactivated with Con A was much lower than that by other cells, suggesting that T cells do not play a major role in ^{18}F -FDG accumulation in synovitis. Furthermore, B cells observed in rheumatoid synovitis often form germinal centers in the region of rheumatoid synovitis and proliferate in situ (29). Because B cells accumulate ^{18}F -FDG under proliferative conditions (30), the involvement of ectopic germinal centers of such proliferating B cells would contribute to ^{18}F -FDG accumulation in rheumatoid synovitis in human RA. In addition, it is known that the extent of ectopic germinal centers in B cells varies among individuals; thus, ^{18}F -FDG accumulation in human RA may be affected by the extent of ectopic germinal centers in B cells. These issues remain to be investigated in future studies.

Our data support the results of previous clinical studies showing that the standardized uptake value correlates with the volume of the pannus evaluated by MRI and US. Our data also show that ^3H -FDG uptake varies depending on the environment of the cells forming the pannus. These results suggest that ^{18}F -FDG accumulation in RA reflects the inflammatory environment that results from the disease activity as well as the volume of the pannus. In clinical examinations of RA, because the activated pannus directly leads to the destruction of articular bone and cartilage, ^{18}F -FDG accumulation in RA may provide important biologic information about future joint destruction; in addition, ^{18}F -

FDG PET may have advantages over MRI or US for evaluation of the disease activity of RA.

CONCLUSION

We evaluated the correlation between ^{18}F -FDG accumulation in arthritis and pathologic findings by using a CIA animal model; we found a higher level of ^{18}F -FDG accumulation in the pannus. The in vitro ^3H -FDG uptake assay with various cells involved in the pannus indicated that fibroblasts predominantly contributed to ^{18}F -FDG accumulation. Additionally, inflammatory conditions, such as inflammatory cytokine production and hypoxia, altered cellular activity or metabolism and enhanced ^{18}F -FDG uptake in fibroblasts and macrophages. Our results suggested that ^{18}F -FDG accumulation in RA reflects the proliferation of the pannus and inflammatory activity. ^{18}F -FDG PET should be effective for quantifying arthritis activity.

ACKNOWLEDGMENT

We thank Dr. Kazuhiko Yamamoto from the Department of Allergy and Rheumatology, Graduate School of Medicine, The University of Tokyo, for valuable discussions. This work was supported in part by a Health Sciences Research Grant for Research on Specific Diseases from the Ministry of Health, Labour, and Welfare, Japan.

REFERENCES

1. Harris ED Jr. Rheumatoid arthritis: pathophysiology and implications for therapy. *N Engl J Med.* 1990;322:1277–1289.
2. Lee DM, Weinblatt ME. Rheumatoid arthritis. *Lancet.* 2001;358:903–911.
3. Scutellari PN, Orzincolo C. Rheumatoid arthritis: sequences. *Eur J Radiol.* 1998;27(suppl 1):S31–S38.
4. Brook A, Corbett M. Radiographic changes in early rheumatoid disease. *Ann Rheum Dis.* 1977;36:71–73.
5. Egsmose C, Lund B, Borg G, et al. Patients with rheumatoid arthritis benefit from early 2nd line therapy: 5 year followup of a prospective double blind placebo controlled study. *J Rheumatol.* 1995;22:2208–2213.
6. McQueen FM. Magnetic resonance imaging in early inflammatory arthritis: what is its role? *Rheumatology (Oxford).* 2000;39:700–706.
7. Beckers C, Ribbens C, Andre B, et al. Assessment of disease activity in rheumatoid arthritis with ^{18}F -FDG PET. *J Nucl Med.* 2004;45:956–964.
8. Polisson RP, Schoenberg OI, Fischman A, et al. Use of magnetic resonance imaging and positron emission tomography in the assessment of synovial volume and glucose metabolism in patients with rheumatoid arthritis. *Arthritis Rheum.* 1995;38:819–825.
9. Beckers C, Jeukens X, Ribbens C, et al. ^{18}F -FDG PET imaging of rheumatoid knee synovitis correlates with dynamic magnetic resonance and sonographic assessments as well as with the serum level of metalloproteinase-3. *Eur J Nucl Med Mol Imaging.* 2006;33:275–280.
10. Renner ED, Plagemann PG, Bernlohr RW. Permeation of glucose by simple and facilitated diffusion by Novikoff rat hepatoma cells in suspension culture and its relationship to glucose metabolism. *J Biol Chem.* 1972;247:5765–5776.
11. Palmer WE, Rosenthal DI, Schoenberg OI, et al. Quantification of inflammation in the wrist with gadolinium-enhanced MR imaging and PET with 2-[^{18}F]-fluoro-2-deoxy-D-glucose. *Radiology.* 1995;196:647–655.
12. Goerres GW, Forster A, Uebelhart D, et al. F-18 FDG whole-body PET for the assessment of disease activity in patients with rheumatoid arthritis. *Clin Nucl Med.* 2006;31:386–390.
13. Kawamoto T. Use of a new adhesive film for the preparation of multi-purpose fresh-frozen sections from hard tissues, whole-animals, insects and plants. *Arch Histol Cytol.* 2003;66:123–143.

14. Feldmann M, Maini RN. Anti-TNF alpha therapy of rheumatoid arthritis: what have we learned? *Annu Rev Immunol.* 2001;19:163–196.
15. Al-Shukaili AK, Al-Jabri AA. Rheumatoid arthritis, cytokines and hypoxia: what is the link? *Saudi Med J.* 2006;27:1642–1649.
16. Gamelli RL, Liu H, He LK, Hofmann CA. Augmentations of glucose uptake and glucose transporter-1 in macrophages following thermal injury and sepsis in mice. *J Leukoc Biol.* 1996;59:639–647.
17. Cornelius P, Marlowe M, Lee MD, Pekala PH. The growth factor-like effects of tumor necrosis factor-alpha: stimulation of glucose transport activity and induction of glucose transporter and immediate early gene expression in 3T3-L1 preadipocytes. *J Biol Chem.* 1990;265:20506–20516.
18. Bird TA, Davies A, Baldwin SA, Saklatvala J. Interleukin 1 stimulates hexose transport in fibroblasts by increasing the expression of glucose transporters. *J Biol Chem.* 1990;265:13578–13583.
19. Taylor PC, Sivakumar B. Hypoxia and angiogenesis in rheumatoid arthritis. *Curr Opin Rheumatol.* 2005;17:293–298.
20. Stevens CR, Williams RB, Farrell AJ, Blake DR. Hypoxia and inflammatory synovitis: observations and speculation. *Ann Rheum Dis.* 1991;50:124–132.
21. Peters CL, Morris CJ, Mapp PI, et al. The transcription factors hypoxia-inducible factor 1alpha and Ets-1 colocalize in the hypoxic synovium of inflamed joints in adjuvant-induced arthritis. *Arthritis Rheum.* 2004;50:291–296.
22. Kubota R, Yamada S, Kubota K, Ishiwata K, Tamahashi N, Ido T. Intratumoral distribution of fluorine-18-fluorodeoxyglucose in vivo: high accumulation in macrophages and granulation tissues studied by microautoradiography. *J Nucl Med.* 1992;33:1972–1980.
23. Yamada S, Kubota K, Kubota R, Ido T, Tamahashi N. High accumulation of fluorine-18-fluorodeoxyglucose in turpentine-induced inflammatory tissue. *J Nucl Med.* 1995;36:1301–1306.
24. Lewis JS, Lee JA, Underwood JC, Harris AL, Lewis CE. Macrophage responses to hypoxia: relevance to disease mechanisms. *J Leukoc Biol.* 1999;66:889–900.
25. Simon LM, Robin ED, Phillips JR, Acevedo J, Axline SG, Theodore J. Enzymatic basis for bioenergetic differences of alveolar versus peritoneal macrophages and enzyme regulation by molecular O₂. *J Clin Invest.* 1977;59:443–448.
26. Murdoch C, Muthana M, Lewis CE. Hypoxia regulates macrophage functions in inflammation. *J Immunol.* 2005;175:6257–6263.
27. Khandwala AS, Gee JB. Factors in glucose oxidation by alveolar macrophages: glucose transport and glycogenolysis. *Chest.* 1975;67(suppl):60S–63S.
28. Borregaard N, Herlin T. Energy metabolism of human neutrophils during phagocytosis. *J Clin Invest.* 1982;70:550–557.
29. Malone DG, Wahl SM, Tsokos M. Immune function in severe, active rheumatoid arthritis: a relationship between peripheral blood mononuclear cell proliferation to soluble antigens and synovial tissue immunohistologic characteristics. *J Clin Invest.* 1984;74:1173–1185.
30. Shozushima M, Tsutsumi R, Terasaki K, Sato S, Nakamura R, Sakamaki K. Augmentation effects of lymphocyte activation by antigen-presenting macrophages on FDG uptake. *Ann Nucl Med.* 2003;17:555–560.